Purdue University
Purdue e-Pubs

Department of Computer Science Technical Reports | Department of Computer Science

2004

Characterizing Overlay Multicast Networks and their Costs

Sonia Fahmyl
Purdue University, fahmy@cs.purdue.edu

Minseok Kwon

Report Number:
04-007

Fahmyl, Sonia and Kwon, Minseok, "Characterizing Overlay Multicast Networks and their Costs" (2004). *Department of Computer Science Technical Reports.* Paper 1591.
https://docs.lib.purdue.edu/cstech/1591

This document has been made available through Purdue e-Pubs, a service of the Purdue University Libraries. Please contact epubs@purdue.edu for additional information.

CHARACTERIZING OVERLAY MULTICAST NETWORKS AND THEIR COSTS

Sonia Fahmy
Minseok Kwon

Department of Computer Sciences
Purdue University
West Lafayette, IN 47907

CSD TR #04-007
February 2004

Characterizing Overlay Multicast Networks and their Costs

Sonia Fahmy and Minseok Kwon
Department of Computer Sciences, Purdue University
West Lafayette, IN 47907–2066, USA
e-mail: {fahmy,kwonm}@cs.purdue.edu

Abstract— Overlay networks among cooperating hosts have recently emerged as a viable solution to several challenging problems, including multicasting, routing, content distribution, and peer-to-peer services. Application-level overlays, however, incur a performance penalty over router-level solutions. This paper characterizes this performance penalty for overlay multicast trees via experimental data, simulations, and theoretical models. We compare three overlay multicast protocols with respect to latency, bandwidth, router degrees, and host degrees. Experimental data and simulations illustrate that (i) the average delay and the number of hops between parent and child hosts in overlay trees generally decrease, and (ii) the degree of hosts generally decreases, as the level of the host in the overlay tree increases. Overlay multicast routing strategies, overlay host distribution, together with power-law and small-world Internet topology characteristics, are identified as causes of the observed phenomena. We show that these phenomena are directly related to the overlay tree cost. Our results reveal that the normalized cost $\frac{L(n)}{U(n)} \propto n^{0.9}$ for small n, where $L(n)$ is the total number of hops in all overlay links, $U(n)$ is the average number of hops on the source to receiver unicast paths, and n is the number of members in the overlay multicast session.

I. Introduction

Overlay networks have recently gained attention as mechanisms to overcome deployment barriers to router-level solutions of several networking problems. Overlay solutions for multicasting [1], [2], [3], [4], [5], inter-domain routing pathologies [6], [7], content distribution [8], and content sharing [9], [10], [11] are being extensively studied. In this paper, we consider a number of *overlay* (application-layer) multicast approaches which have been proposed over the last three years. In overlay multicast, hosts participating in a multicast session form an overlay network, and only utilize unicasts among pairs of hosts (considered neighbors in the overlay tree) for data dissemination. The hosts in overlay multicast exclusively handle group management, routing, and tree construction, without any support from Internet routers.

The key advantages overlays offer are flexibility, adaptivity, and ease of deployment. Overlays, however, impose a performance penalty over router-level alternatives. While overlay multicast clearly consumes additional network bandwidth and increases latency over IP multicast, little attention has been paid to precisely quantifying this overlay performance penalty, either theoretically or experimentally. Moreover, to the best of our knowledge, there is no work on characterizing overlay multicast tree structure. Such characterization is important to gain insight into overlay properties and their causes at *both* the application layer and the underlying network layer. It is also important to compare different overlay multicast strategies to determine how to meet the goals of target applications (e.g., by balancing latency versus bandwidth tradeoffs).

In this paper, we analyze overlay multicast trees via (i) real data integrated from End System Multicast (ESM)/Narada [1] experiments and traceroute servers, (ii) simulations of three representative classes of overlay multicast strategies, and (iii) simple analytical models. We quantify several aspects of the performance penalty associated with overlay multicast, with emphasis on the overlay cost (i.e., efficiency) at the network-layer. We derive and validate asymptotic forms of the overlay cost from two different tree models.

Our results indicate that (i) the average delay and the number of hops between parent and child hosts generally decrease, and (ii) the degree of hosts generally decreases, as the level of the host in the overlay tree increases. We find that overlay multicast routing strategies, overlay host distribution, *together with* power-law and small-world Internet topology characteristics, are causes of these observed phenomena. We isolate the impact of each of these causes, and quantify its effect on the overlay cost. Our results reveal that the normalized overlay cost $\frac{L(n)}{U(n)} \propto n^{0.9}$ for small n, where $L(n)$ is the total number of hops in all overlay links (connections), $U(n)$ is the average number of hops on the source to receiver unicast paths, and n is the number of members in the overlay multicast session. This can be compared to an IP multicast cost proportional to $n^{0.6}$ to $n^{0.8}$ [12], [13].

The remainder of this paper is organized as follows. In Section II, we describe overlay networks and their performance metrics. In Section III, we characterize overlay multicast networks via simulations and experimental data analysis. In Section IV, we propose and validate an overlay multicast model based on our observations. In Section V, we discuss related work. Finally, we summarize our conclusions and future work in Section VI.

II. Overlay Networks: Definitions and Metrics

We consider the *underlying network* as a graph $G = (N, E)$, where N is a set of nodes, and E is a set of edges.

– This research has been sponsored in part by NSF grant ANI-0238294 (CAREER), the Purdue Research Foundation, and the Schlumberger Foundation technical merit award.

A node $\eta_i \in N$ denotes a *router*, and an edge $(\eta_i, \eta_j) \in E$ denotes a bi-directional physical link in the underlying network. An *overlay network* superimposed on G is a *tree* $o = (s, D, N_o, E_o)$, where s is the source host, D is the set of receiver hosts, $N_o \subseteq N$ is the set of nodes in the underlying network G that are traversed by overlay links, and E_o is the set of overlay links, defined below.

The set of hosts H_o consists of s and D in o, i.e., $H_o = \{s\} \cup D$. The cardinality of set H_o is equal to n. An overlay link $e_o = (d_s, \eta_0, \ldots, \eta_{ls}, d_r) \in E_o$ comprises a host $d_s \in H_o$, followed by a sequence of routers $\eta_i \in N_o$, followed by a host $d_r \in D$. Each receiver $\in D$ appears exactly once at the *end* of any sequence denoting an overlay link, but may appear multiple times at the *beginning* of sequences for different overlay links. An overlay link is typically a UDP or TCP connection established by the overlay multicast protocol.

The number of hops in the router sequence $\eta_0, \ldots, \eta_{ls}$ in an overlay link $e_o \in E_o$ is denoted by ls. For every two routers $\eta_i, \eta_j \in N_o$ that appear consecutively in an overlay link $e_o \in E_o$, there must exist a link connecting them in the underlying network, i.e., edge $(\eta_i, \eta_j) \in E$ holds. The same router $\eta_i \in N_o$ can appear in multiple overlay links $e_o \in E_o$. Subsequences of routers $\eta_i, \ldots, \eta_j$ can also appear in multiple overlay links $e_o \in E_o$. Figure 1 illustrates an example overlay network with 6 overlay links.

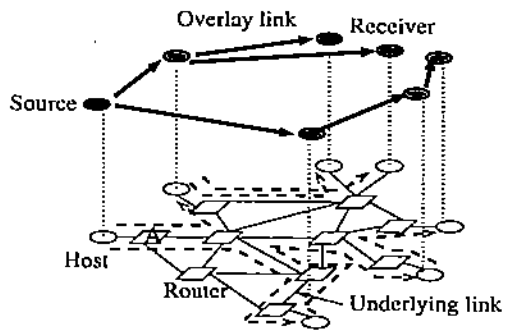

Fig. 1. An example overlay multicast tree over an underlying network

Given an overlay network o, we define the term *overlay cost* as the number of underlying hops traversed by every overlay link $e_o \in E_o$ for an overlay o. More formally, the overlay cost is: $\forall e_o \in E_o$, $\Sigma\ ls(e_o)$, where $ls(e_o)$ denotes the number of router-to-router hops between $\eta_0, \ldots, \eta_{ls}$ for the overlay link e_o (as defined above). We consider the first and last hops to/from hosts separately. This is because we must fairly compare the normalized overlay cost to the normalized IP multicast cost computed in [13], [14], [15], where the first and last hops are ignored. For example, the overlay cost for the overlay in Figure 1 is 2+3+1+1+4+2=13.

We also use the term *link stress* to denote the total number of identical copies of a packet over the same underlying link (as defined in [1], [16]). For example, the stress of the link from the source to A in Figure 1 is two. It is clear that the overlay cost defined above can be represented as $\forall i, \sum_i stress(i)$ where i is any *router-to-router* link traversed by one or more overlay links $e_o \in E_o$, and $stress(i)$ is the stress of link i. Prior work also used a "resource usage" metric, defined as $\forall i$, $\sum_i delay(i) \times stress(i)$, where i is an underlying link traversed by one or more overlay links [1]. Our overlay cost metric is a special case of this resource usage notion, when $delay(i) = 1, \forall i$. We opt to evaluate delays separately from the overlay cost, in order to isolate the delay and stress aspects of an overlay.

In addition to the overlay cost and link stress, we study the following overlay tree metrics: (1) degree of hosts H_o (equivalent to the host contribution to the link stress of the host-to-first-router link), (2) degree of routers $\in N_o$, and hop-by-hop delays of underlying links traversed by overlay links $\in E_o$, (3) overlay tree height, (4) delays and number of hops between parent and child hosts, (5) mean bottleneck bandwidth between the source s and receivers $\in D$, and (6) mean latency, longest latency, and relative delay penalty (RDP) from the source to a receiver.

The latency $latency(s, d_r)$ from the source s to $d_r \in D$ is: $delay(s, d_0) + \sum_{i=0}^{l-1} delay(d_i, d_{i+1}) + delay(d_l, d_r)$, assuming s delivers data to d_r via the sequence of hosts $(d_0, \cdots, d_l)$. Here, $delay(d_i, d_{i+1})$ denotes the end-to-end delay of the overlay link from d_i to d_{i+1}, for $d_i \in H_o$ and $d_{i+1} \in D$. Note that the RDP from s to d_r (defined in [16]) is the ratio $\frac{latency(s,d_r)}{delay(s,d_r)}$. We compute the mean RDP of all receivers $\in D$. We can also define the *stretch* as $\frac{hops(s,d_r)}{ls(s,d_r)+2}$ where $hops(s, d_r) = ls(s, d_0) + \sum_{i=0}^{l-1}(ls(d_i, d_{i+1}) + 2) + ls(d_l, d_r) + 4$. Stretch denotes the relative number of hops instead of the relative latency used in RDP. These metrics compare overlay multicast to unicast (or IP multicast using a minimum delay tree). It is clear that there is a tradeoff between the latency metrics and the stress/bandwidth metrics. Balancing this tradeoff is the key to effective overlay multicast protocol design.

III. Overlay Multicast Tree Structure

Our primary goal in this section is to isolate the impacts of (i) the overlay protocol, (ii) the underlying network connectivity and routing, and (iii) the overlay host distribution, on the overlay tree structure. We first analyze experimental data, and then conduct a set of simulations.

A. Experimental Data

In order to study the structure of *real* overlay networks in the Internet, we analyze experimental results for the End System Multicast (ESM) protocol [1], [16], the TAG protocol [4] and the NICE protocol [3]. To analyze ESM, we recorded the overlay trees constructed during experiments performed by the ESM developers in November 2002. (Unfortunately, the ESM developers have not released the overlay tree structure in their later experiments.) Since the overlay trees did not change significantly throughout the experiment lifetime, we selected one representative overlay tree. The tree comprises 65 hosts.

We use *traceroute* to find the underlying path between every

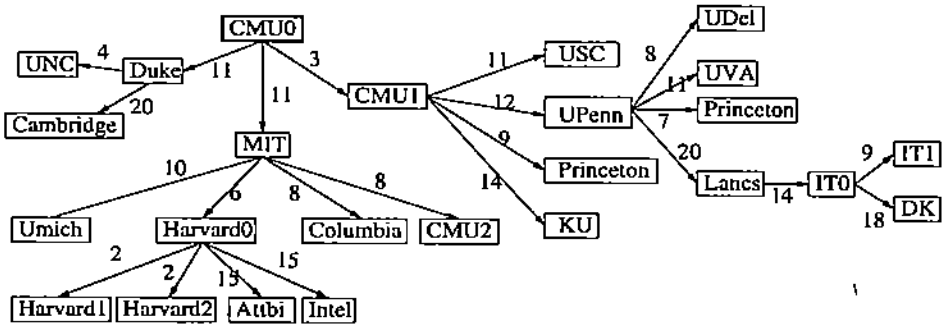

Fig. 2. A part of the overlay tree constructed by End System Multicast in November 2002. The number next to the overlay link denotes the hop count between parent and child hosts.

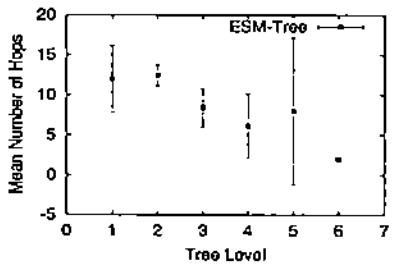

(a) Number of router-to-router hops between parent-child hosts versus level of host in overlay tree

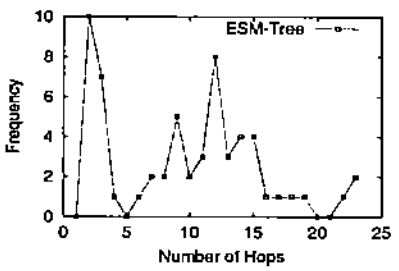

(b) Frequency of occurrence of number of hop values between parent-child hosts

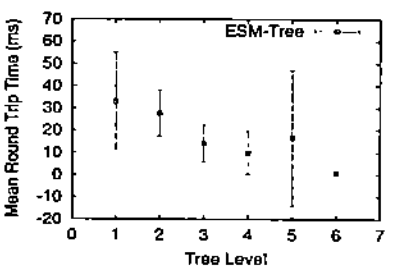

(c) Mean round trip time between parent-child hosts versus level of host in overlay tree

Fig. 3. Overlay trees constructed by End System Multicast in November 2002

two hosts on the overlay tree. We encountered two problems using traceroute. First, some routers do not generate ICMP Time-Exceeded packets when TTL (Time-To-Live) reaches zero. Second, many routers disable the source-route capability, primarily due to security concerns. Due to this, finding paths between two arbitrary hosts via traceroute (without having accounts on either of these hosts) becomes difficult. We utilize publicly available traceroute servers [17] and our own machines to compute paths to all the hosts on the overlay tree. These paths are then synthesized to approximate the paths between any two overlay hosts. Our task was simplified because the hosts in the experiments, with a few exceptions, are located at universities in the United States. Most university hosts are connected to the Internet2 backbone network [18], and thus the routes typically intersect at points on Internet2. These points provide the synthesis junctions used for path extraction. A part of the synthesized overlay tree is depicted in Figure 2.

Figure 3(a) depicts the mean number of hops between every two parent-child ESM hosts, for hosts at different levels of the overlay tree (90% confidence intervals are shown to indicate variability). The figure shows that the number of hops typically decreases as the host level increases, though the decrease is not monotone. We now seek the causes of this phenomenon. Consider a set of routers that are connected according to the power-law [19] and small-world [20], [21] properties. The power-law property dictates that there is a larger number of low-degree routers than high-degree routers. We surmise that a high-degree high-bandwidth router is typically more likely to be traversed by overlay links near the source of the overlay tree. This is because a high-degree router has higher chances of reducing the path length and delays than a low-degree router, due to its connectivity to a larger number of routers. The high-degree router is also more likely to have high bandwidth links connected to it. Overlay multicast protocols which consider delay, path length, or bandwidth are thus likely to exploit such high-degree routers in the first few levels of the tree (unless all hosts are clustered near the source). Recall also that nearby hosts tend to be clustered by the small-world property. Accordingly, we can visualize an overlay tree where a number of high-degree routers connect the hosts at the first few levels of the tree. In addition, many hosts are connected to low-degree lower-bandwidth routers, which are clustered at lower levels of the tree. Therefore, hosts at lower levels of the overlay tree may only be a few hops away from each other.

In Figure 3(b), we plot the frequency of occurrence of certain numbers of hops between parent-child ESM hosts. The figure shows that a significant number of hosts are within 2 or 3 hops of their parents, and many are 9–15 hops away. The distribution of round trip times between every two parent-child

ESM hosts at different levels of the overlay tree is plotted in Figure 3(c) (with 90% confidence intervals). We use round trip time estimates obtained from traceroute. From the figure, the average round trip time generally decreases as the host level increases, confirming our intuition. The large error ranges in the figure indicate that the round trip times significantly vary at the same level of the tree.

Figure 4 shows the distribution of per-hop delay (the delay between two consecutive routers on a path from a parent to a child ESM host) for different overlay tree levels. The per-hop delay between two consecutive routers η_i and η_j is estimated as $\frac{1}{2}rtt(\eta_i, \eta_j)$, where $rtt(\eta_i, \eta_j)$ is the time to travel from η_i to η_j and vice versa obtained via traceroute. The figure indicates that 78% of per-hop delays in lower tree levels (levels 4-6) are shorter than 0.25 ms, and only 2% are between 2.5 and 5 ms. In contrast, only 44% of per-hop delays are shorter than 0.25 ms, 11% are between 2.5 and 5 ms, and 15% exceed 5 ms, for the first level of the tree, which agrees with our earlier explanation. Figure 5 illustrates that the degree of hosts in the overlay tree grows as hosts get closer to the root of the overlay tree. This decreasing degree can be attributed ESM's goal of minimizing delay (if bandwidth is acceptable).

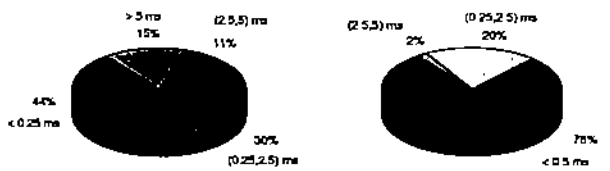

(a) Tree level 1 (b) Tree level 4-6

Fig. 4. Distributions of per-hop delay for different overlay tree levels

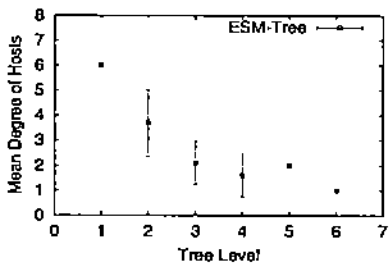

Fig. 5. Degree of host versus level of host in overlay tree constructed by End System Multicast in November 2002

We have also conducted experiments with NICE [3] and TAG [4] on the PlanetLab testbed [22]. We use *tracepath* [23] to find the number of hops and delay on underlying paths. We selected representative overlay trees for NICE and TAG from several experiments with 60 group members. A cluster in NICE has 2 to 5 members (see [3] for details). For TAG, we use $bwthresh = 160$ kbps, $chlimit = 5$, and $u = 1$ (the details of the TAG algorithm and its parameters are discussed in Section III-B.1). Figure 6 depicts the mean number of hops between parent-child hosts (we do not show variability in the remainder of the paper). The tree constructed by NICE does not exhibit the same decrease in number of hop as tree level increases exhibited by ESM and TAG. This is because scalability is the primary concern of NICE, and not bandwidth or delay as in ESM and TAG. In Figure 7, we also show the delay between parent-child hosts for different overlay tree levels. We compute the delay by halving the round trip times between parent-child hosts.

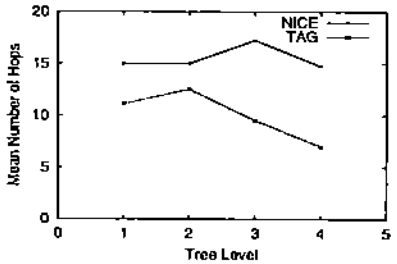

Fig. 6. Mean number of router-to-router hops between parent-child hosts versus level of host in overlay trees constructed by NICE and TAG on PlanetLab

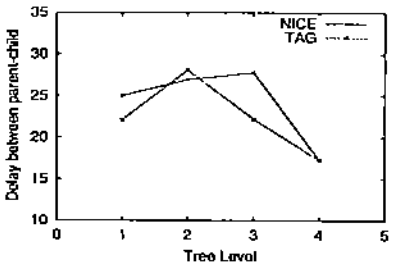

Fig. 7. Delay between parent-child hosts versus level of host in overlay trees constructed by NICE and TAG on PlanetLab

B. Simulation Experiments

We also investigate the overlay structure via simple session-level simulations.

B.1 Simulation Setup

We use two router-level topologies. The first topology contains 4000 routers connected according to power-law and small-world properties. In a power-law distribution, a complementary cumulative distribution function $cd^{-\alpha}$ is used to denote the fraction of routers with degree greater than d, where c and α are constants [24], [25]. We use $c = 1$ and $\alpha = 1.22$. Groups of routers are clustered according to the small-world property: a router connects to its closest neighbor routers with probability p, and to other routers with probability $1 - p$, according to router degree. We use $p = 0.5$. Routers are uniformly distributed on a 750×750 plane, and the Euclidean distance between two routers approximates the delay between the two routers (in ms). Hosts are connected to edge routers (which are defined as routers with degree less than 10) uniformly at random. The bandwidth from edge routers to hosts

is selected according to the realistic distribution: 40% are 56 kbps, and 15% for each of 1.5, 5, 10, 100 Mbps. All other links are assigned bandwidths ranging from 100 Mbps to 1 Gbps.

The second topology we use is a Transit-Stub topology generated by the popular GT-ITM topology generator [26]. The topology contains 4040 routers which constitute 4 transit domains, 10 routers per transit domain, 4 stub domains per transit router, and 25 routers per stub domain. GT-ITM generates symmetric link delays ranging from 1 to 55 ms for transit-transit or transit-stub links. We use 1 ms to 10 ms delays within a stub. Hosts are connected to stub routers randomly and uniformly. Backbone links have bandwidths ranging from 100 Mbps to 1 Gbps, while links from edge routers to hosts have the same bandwidth range as in the first topology. In both topologies, the underlying network routes are selected to optimize *delays*. It is also worth mentioning that we have simulated smaller scale topologies and the results were similar.

Algorithm 1 End System Multicast (ESM)

A new member $d \in H_o$ joins a session
$NE_d = \emptyset$
d probes d_j ($\neq d$) $\in H_o - NE_d$ randomly and periodically forming M_o
for all d_i ($\neq d$) $\in H_o$ do
  CB = current bandwidth level between d and d_i
  NB = new bandwidth level between level d and d_i via d_j
  CL = current latency between d and d_i
  NL = new latency between d and d_i via d_j
  if $NB > CB$ then
    $utility$ += 1
  else if $NB = CB$ and $NL < CL$ then
    $utility$ += $\frac{CL-NL}{CL}$
  end if
end for
if $utility$ > addthresh and degree(d) < UDB and degree(d_j) < UDB then
  $NE_d = NE_d \cup \{d_j\}$
end if
Current members exchange routing information on M_o
When d receives a table of (bwl(d_n,d_i), latency(d_n,d_i), d_n) from $d_n \in NE_d$ for all $d_i \in H_o$
for all d_i ($\neq d$) $\in H_o$ do
  if bwl(d,d_i) < min(bwl(d,d_n), bwl(d_n,d_i)) then
    d_n is a new next hop from d to d_i. Routing information is updated accordingly
  else if bwl(d,d_i) == min(bwl(d,d_n), bwl(d_n,d_i)) then
    if latency(d,d_n)+latency(d_n,d_i) < latency(d,d_i) then
      d_n is a new next hop from d to d_i. Routing information is updated accordingly
    end if
  end if
end for

{$addthresh$ is the threshold for adding neighbors, UDB is the upper degree bound, bwl(d_i,d_j) indicates the bandwidth level between d_i and $d_j \in H_o$, and latency(d_i,d_j) denotes the latency between d_i and $d_j \in H_o$, where M_o = overlay mesh, H_o = set of hosts on M_o, and NE_d = set of current neighbors of $d \in H_o$ on M_o.}

We simulate three representative overlay multicast protocols on the two topologies: ESM [1], Topology-Aware Grouping (TAG) [4], and Minimum Diameter Degree-Bounded Spanning Tree (MDDBST) [5]. The reason we select ESM is

Algorithm 2 TAG(C,N) where C represents a currently examined node and N is a new member

$target \leftarrow C$, $ch \leftarrow$ first child of C
if $ch = NULL$ then
  add N to the children of C
  return
end if
while $ch \neq NULL$ do
  if len(P(S,N)) $\geq$ len(P(S,ch)) and commonpath(ch,N) $\geq$ max(len(P(S,ch))-u,0) then
    $target \leftarrow ch$
    break
  end if
  $ch \leftarrow$ next child of C
end while
if $target \neq C$ then
  TAG($target$,N)
else
  if bandwidth(C)>$bwthresh$ and chdnum(C)<$chlimit$ then
    add N to the children of C
  else
    $target_1 \leftarrow C$, $target_2 \leftarrow C$, $target_3 \leftarrow C$
    $l \leftarrow$ len(P(S,C)), $maxbw_2 \leftarrow$ bandwidth(C), $maxbw_3 \leftarrow$ bandwidth(C)
    for all ch such that ch is a child of C do
      if commonpath(ch,N)>l and bandwidth(ch)>$bwthresh$ and chdnum(ch)<$chlimit$ then
        $target_1 \leftarrow ch$, $l \leftarrow$ commonpath(ch,N) {priority rule 1}
      else if bandwidth(ch)>$maxbw_2$ and chdnum(ch)<$chlimit$ then
        $target_2 \leftarrow ch$, $maxbw_2 \leftarrow$ bandwidth(ch) {priority rule 2}
      else if bandwidth(ch)>$maxbw_3$ then
        $target_3 \leftarrow ch$, $maxbw_3 \leftarrow$ bandwidth(ch) {priority rule 3}
      end if
    end for
    if $target_1 \neq C$ then
      $target \leftarrow target_1$
    else if $target_2 \neq C$ then
      $target \leftarrow target_2$
    else if $target_3 \neq C$ then
      $target \leftarrow target_3$
    end if
    if $target = C$ then
      for all ch such that ch is a child of C and len(P(S,ch)) $\geq$ len(P(S,N)) and commonpath(N,ch) $\geq$ max(len(P(S,N))-u,0) do
        add ch to the children of N
      end for
      add N to the children of C
    else
      TAG($target$,N)
    end if
  end if
end if

{**Functions:**
  len(P(S,A)): length of the path from the root S to A
  chdnum(A): number of the children of A
  bandwidth(A): available bandwidth between A and N
  commonpath(A,B): length of common prefix between the spaths of A and B
  max(A,B): maximum of A and B
Variables:
  $bwthresh$: bandwidth threshold
  $chlimit$: upper bound on the number of children
  ch: child of C
  l: length of the longest common prefix between the spaths of ch and N
  $target$: node that N will examine next
  $target_i$: next node computed according to priority rule i
  $maxbw_i$: maximum bandwidth(A) according to priority rule i}

Algorithm 3 Minimum Diameter Degree-Bounded Spanning Tree (MDDBST)

```
for all v ∈ V do
  δ(v) = c(src, v)
  p(v) = src
  d_max(v) = lastbw(v)/unitbw
end for
T = (W = {src}, L = {})
while W ≠ V) do
  let u ∈ V − W be the vertex with smallest δ(u)
  W = W ∪ {u}, L = L ∪ {{u, p(u)}}
  for all v ∈ W − {u} do
    δ(v) = max{δ(v), dist_T(u, v)}
  end for
  for all v ∈ V − W do
    δ(v) = ∞
    for all q ∈ W do
      if degree(q) < d_max(q) and c(v, q) + δ(q) < δ(v)) then
        δ(v) = c(v, q) + δ(q), p(v) = q
      end if
    end for
  end for
end while
```

{$c(u,v)$ = edge cost for $u,v \in V$, $degree(v)$ = degree of $v \in V$, $lastbw(v)$ = last hop bandwidth of $v \in V$, and $unitbw$ = bandwidth constraint for a single connection}

that it is the first overlay multicast protocol to be widely tested in the Internet. It was used for multicasting the SIGCOMM 2002/2003 conferences. Moreover, ESM has a unique routing mechanism. The overlay tree construction protocol of ESM is summarized in Algorithm 1. Each host evaluates the utility of other hosts to determine its neighbors. A host has an upper degree bound (UDB) on the number of its neighbors. We use a value of 6 for the upper degree bound. The ESM flavor used in our simulations has two discretized bandwidth levels: $>$ 100 kbps and $\leq$ 100 kbps (similar to the version used for the SIGCOMM 2002 multicast). The overlay tree is first optimized for bandwidth, and then uses delay as a tie breaker among hosts at the same bandwidth level.

The second class of protocols we investigate is topology-aware overlay multicast protocols, which includes Scribe [27], topology-aware Content-Addressable Network (CAN) [28], and TAG [4]. We select TAG as a representative of this group. TAG is a faithful representation of topology-based approaches, since it aligns overlay routes and underlying routes, if certain weak constraints are met. Although the TAG heuristic may not perform particularly well if inter-domain routes are of poor quality, its simplicity makes it appealing. The pseudo-code for TAG tree construction is given in Algorithm 2. A TAG host becomes the child of the host that most "matches" its path. Here, a path is defined as the sequence of routers from the source to a host. A's path matches B's path when the path from the source to A and the path from the source to B have a common prefix of length equal to the path from the source to A minus u unmatched routers. Two weak constraints are employed by TAG on the bandwidth and the number of children of a host (the bandwidth from a parent to a new member is larger than $bwthresh$ and the number of children of the parent is less than $chlimit$). We use $u = 0$, $bwthresh$= 150 kbps and $chlimit = 50$ in our simulations.

The third class of protocols we investigate includes protocols that seek to minimize overlay cost [29], or the longest path in an overlay network [5] (with delay or bandwidth constraints). We select MDDBST, given in [5], as a representative protocol in this class. MDDBST minimizes the cost (delay in our simulations) in the longest path, and bounds the degree of hosts. The pseudo-code for MDDBST is presented in Algorithm 3. The MDDBST protocol we use is slightly modified for use in a single-source overlay multicast scenario. We define the degree bound as $degree(v) = lastbw(v)/unitbw$, where $degree(v)$ is the degree of node v, $lastbw(v)$ is the last hop bandwidth of v, and $unitbw$ is the desired bandwidth for a single connection. We use $unitbw = 56$ kbps in our simulations. For each protocol, we run five simulations with different random number generator seeds (for topology generation and for selecting the multicast source and destinations) and average the results.

Table I compares a number of overlay multicast algorithms with respect to tree construction, tree types, tree height, group size, metrics, and control overhead.

B.2 Simulation Results

Figure 8 illustrates the mean number of hops between parent and child hosts for different host levels in the overlay tree The labels "ESM-40", "ESM-400" and "ESM-4k" denote ESM with 40, 400, or 4000 members respectively, and so on. Figure 8(a) depicts the results on the power-law and small-world topology. The figure reveals that the number of hops between parent and child hosts tends to decrease as the level in the overlay tree increases, for both ESM and TAG. MDDBST does not exhibit a clear trend. The observed decrease in mean number of hops is consistent with our experimental data, and our intuition on the effect of Internet topology characteristics.

In order to isolate the effects of the power-law property from the small-world property, we execute the same simulations on only-power-law (but no clustering) and only-small-world (but equal degree routers) topologies. Figures 8(b) and 8(c) give the results. From both figures, we observe that the number of hops in ESM and TAG decreases with overlay tree level increase. Therefore, *both* clustering among closely located routers as dictated by the small-world property, and power-laws of router degrees, contribute to the observed decrease in number of hops with overlay tree level increase.

Figure 9 depicts the results on the GT-ITM Transit-Stub topology. ESM shows slightly less noticeable and less rapid decrease in the number of hops as the level increases compared to Figure 8(a). This is expected since GT-ITM router degrees do *not* follow a power-law. TAG is similar in both Figures 8(a) and 9. For MDDBST, the number of hops between parent and child hosts initially fluctuates and slowly decreases as the level increases in Figure 9. This is because MDDBST does not seek the shortest path to individual hosts, but minimizes the longest path. In general, the decreases are more pronounced for TAG

TABLE I

A COMPARISON OF OVERLAY MULTICAST ALGORITHMS

Algorithm	Mesh/Tree	Tree type	Tree height	Group size	Metrics	Control overhead
ESM	Mesh	Source	Unbounded	Small	Bandwidth, delay	O(n)
NICE	Implicit	Source	$O(\log n)$	Large	Delay	$O(\log n)$
Overcast	Tree	Source	Unbounded	Large	Bandwidth	O(max-degree)
CAN-multicast	Implicit	Source	$O(dn^{1/d})$	Large	Delay	Constant
ScatterCast	Mesh	Source	Unbounded	Large	Delay	O(max-degree)
Yoid	Tree	Shared	Unbounded	Large	Delay	O(max-degree)
ALMI	Tree	Shared	Unbounded	Small	Delay	O(max-degree)
MDDBST	Tree	Shared	Unbounded	Large	Edge cost	O(max-degree)
Scribe	Implicit	Source	$O(\log n)$	Large	Delay	$O(\log n)$
HMTP	Tree	Shared	Unbounded	Large	Delay	O(max-degree)
Hypercast	Mesh	Source	Unbounded	Large	Coordinate, angle	O(max-degree)
TAG	Tree	Source	Unbounded	Large	Delay, bandwidth	O(max-degree)
Bayeux	Implicit	Source	$O(\log n)$	Large	Delay	$O(\log n)$

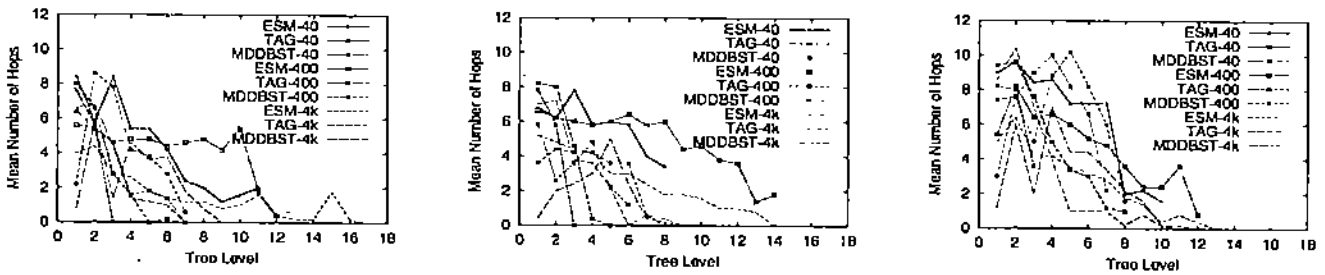

(a) Power-law and small-world topology (b) Only-power-law topology (c) Only-small-world topology

Fig. 8. Mean number of parent-child hops versus overlay tree level in power-law and small-world simulations

than for the other two protocols, independent of underlying topologies, since TAG aligns overlay and underlying routes (subject to bandwidth availability).

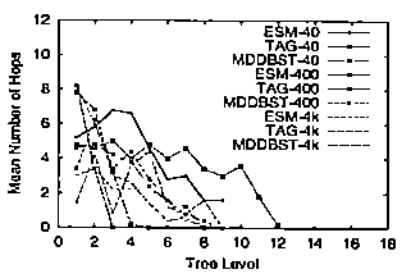

Fig. 9. Mean number of parent-child hops versus overlay tree level in GT-ITM Transit-Stub simulations

We also simulate the three protocols on the power-law and small-world topology with a *non-uniform* host distribution. In this case, we randomly select an edge router and then connect ω hosts to this router and its neighboring routers (one host per router), where ω is a random number between 1 and 20. Figure 10 illustrates that the number of hops between parent and child hosts decreases even more rapidly (though

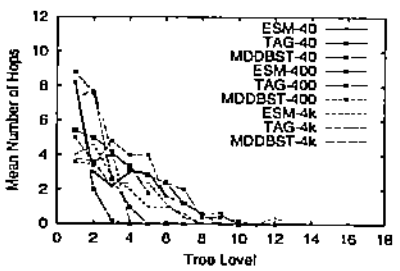

Fig. 10. Distributions of the number of hops versus overlay tree level in simulations on the power-law and small-world topology with non-uniform host distribution

with some fluctuations) than uniform host distribution case (Figure 8(a)). The decrease was less pronounced when we repeated the same experiment on the Transit-Stub topology. Therefore, the power-law and small-world properties, and the non-uniform host distribution are all factors that exacerbate this phenomenon. The routing features of overlay multicast protocols, such as the utility for selecting neighbors in ESM, or topology awareness in TAG, also play an important role.

To validate our argument that high-degree routers tend to be

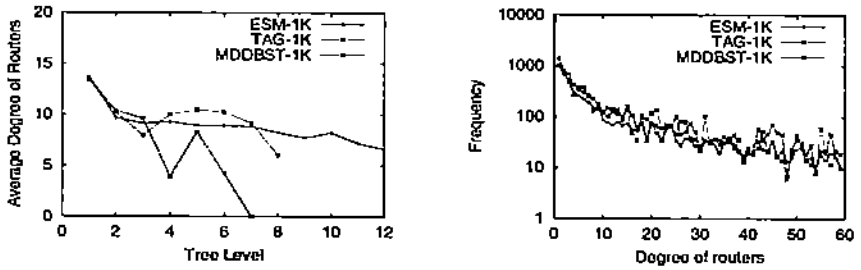

(a) Router degree versus overlay tree level of destination host

(b) Router degree versus frequency

Fig. 11. Router degree in simulations on the power-law and small-world topology

traversed in upper levels of the overlay tree, we plot the distribution of the router degree against the overlay tree level for the power-law and small-world topology (Figure 11(a)). The router degree denotes the connectivity of the router to other *routers*. For tree level i, the routers on overlay links from hosts at level $i-1$ to i are considered. (Note that the same router may appear at different levels of the overlay tree, if traversed by overlay links at different levels). The results agree with our argument. In Figure 11(b), we plot the frequency that routers with certain degrees are traversed by overlay links. The figure shows that all three protocol trees cross a significant number of high-degree routers (50+), in order to exploit their high connectivity and high bandwidth.

In addition, we have investigated the distribution of the host degree against the host overlay tree level for the power-law and small-world topology. The host degree remains within a small range ($\leq$ 20), except for the source and few high-bandwidth hosts in the case of the TAG protocol. This is because TAG attempts to send more copies from the source or high-bandwidth hosts to reduce delay when all receivers are far from each other. As a result, the ESM and MDDBST trees are longer than TAG trees. The tree height increases as the number of members is increased, but the increase is slow beyond a certain number of members. We have also studied the total stress for all three protocols, and found that ESM exhibits the lowest stress, followed by MDDBST, then TAG. The total stress is computed as $\sum_i stress(i)$ where i is any *router-to-router* link or *host-to-router* link traversed by overlay links.

Figure 12 depicts the mean and longest latencies, and the relative delay penalty (RDP) (defined in Section II) for the power-law and small-world topology. ESM achieves the lowest mean latencies and RDP when the number of members is large. ESM, however, exhibits the highest longest latency (Figure 12(b)). The mean latency and RDP for ESM decrease for large groups because, as more hosts join (and since they are randomly located), lower latency paths may become available. In contrast, TAG exhibits low mean latencies and RDP for a small number of members. Although MDDBST exhibits higher mean latencies and RDP, the longest latencies of MDDBST are low, as expected, since MDDBST minimizes diameter.

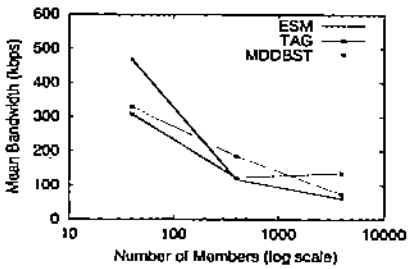

Fig. 13. Mean bottleneck bandwidth in simulations on the power-law and small-world topology

The mean bottleneck bandwidth between the source and receivers for all three protocols is illustrated in Figure 13. The receivers in ESM obtain higher bandwidth than the receivers in TAG because ESM considers bandwidth as a primary metric. The bandwidth of the three protocols decreases as more members join, as expected. Figures 12(a) and 13 together illustrate the latency versus bandwidth tradeoff in ESM. Note that these results may vary with protocol parameters. For example, TAG gives lower RDPs and lower bandwidths with a smaller u or a smaller $bwthresh$. MDDBST can also increase bandwidth with a lower degree bound, at the expense of longer latency and RDP values.

To further investigate the effects of underlying topology, we vary the power-law and small-world parameters, specifically α and the probability p. In Figure 14(a), we find that the number of hops in all three protocols decreases slowly with overlay tree level increase, when router degrees have a wide range. Relay through high-degree routers may reduce the number of hops between hosts in this case. As the range of router degrees becomes narrow (Figure 14(c)), the number of hops tends to fluctuate. Figure 15 shows that a stronger small-world effect yields slightly more rapid decrease of the number of hops. We also observe the effects of different overlay host distributions in Figure 16. Non-uniform host distribution results in a more pronounced decrease. Results of experiments on the three protocols with different parameters are shown in Figure 17. The

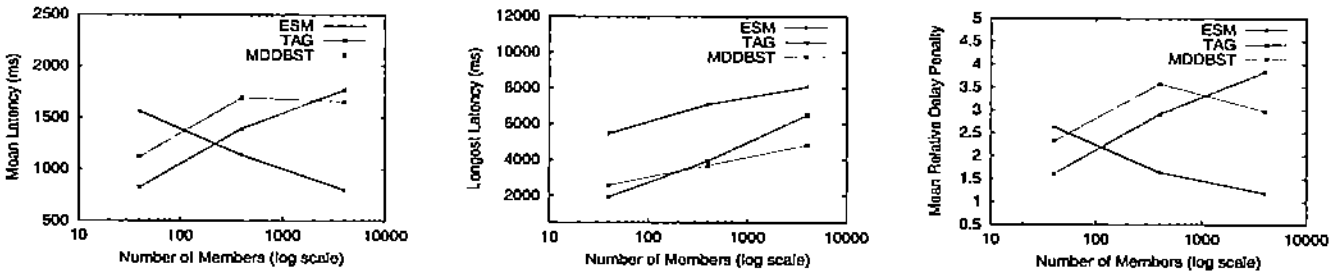

(a) Mean latency (b) Longest latency (c) Mean relative delay penalty

Fig. 12. Mean and longest latency, and mean relative delay penalty (RDP) in simulations on the power-law and small-world topology

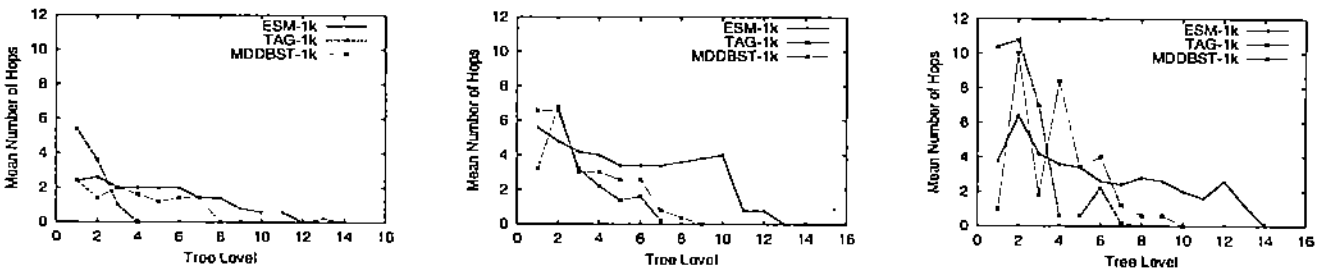

(a) ($\alpha = 0.5, p = 0.5$) (b) ($\alpha = 1.22, p = 0.5$) (c) ($\alpha = 2, p = 0.5$)

Fig. 14. Mean number of parent-child hops versus overlay tree level as the effect of power-law decreases

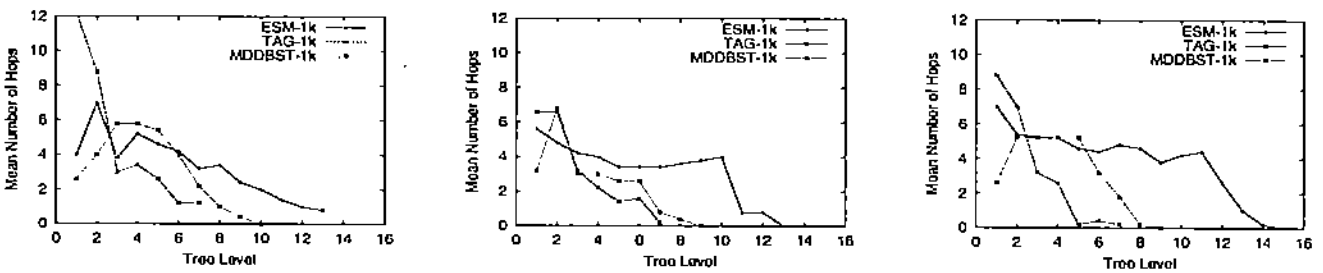

(a) ($\alpha = 1.22, p = 0.9$) (b) ($\alpha = 1.22, p = 0.5$) (c) ($\alpha = 1.22, p = 0.1$)

Fig. 15. Mean number of parent-child hops versus overlay tree level as the effect of small-world decreases

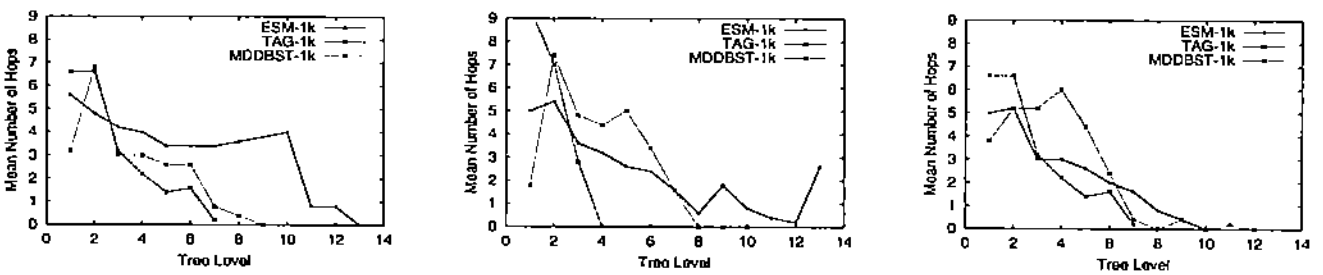

(a) Uniform (b) Cluster of 10 hosts (c) Cluster of 20 hosts

Fig. 16. Mean number of parent-child hops versus overlay tree level for different host distributions

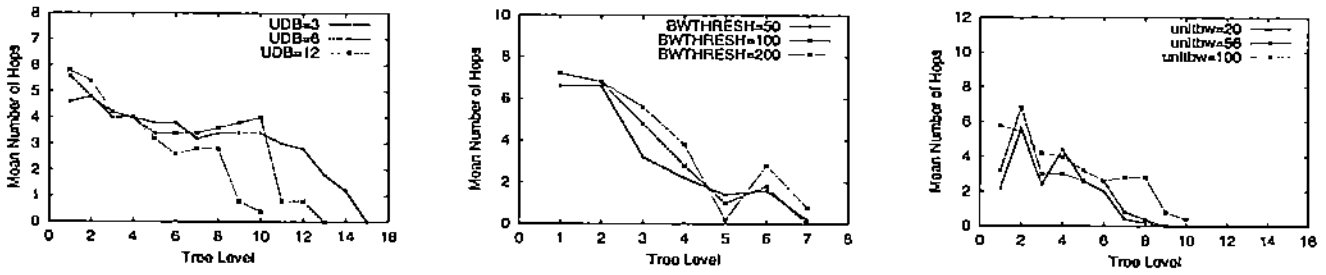

(a) ESM-1k (b) TAG-1k (c) MDDBST-1k

Fig. 17. Mean number of parent-child hops versus overlay tree level with different overlay protocol parameters

parameters result in some differences, though the impact is not very pronounced.

In addition, we compare the normalized overlay costs of different topologies and host distributions. Figure 18(a) and (b) show that a strong power-law (a) or small-world (b) topology achieves lower costs than GT-ITM. Non-uniform host distribution also reduces overlay multicast cost, as depicted in Figure 18(c). These results confirm our intuition that the overlay protocol, the Internet power-law property, the Internet small-world property, and overlay host clustering all contribute to the decrease in the number of hops between parent and child hosts as the overlay tree level increases.

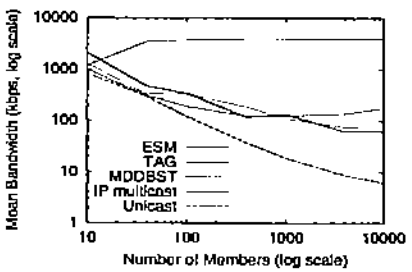

Fig. 19. Bandwidth of IP multicast, unicast and overlay multicast (log-log scale)

Figure 19 compares the mean bandwidth of IP multicast, unicast and overlay multicast. As expected, IP multicast gives the highest mean bandwidth for all experiments with different numbers of members. Overlay multicast yields more bandwidth than naive unicast as the number of members exceeds 100.

IV. Overlay Multicast Tree Cost

In this section, we model overlay multicast trees based on the overlay tree structure we have observed, and compute their costs.

A. Network Model

We model the underlying network as a graph $G = (N, E)$ and the overlay tree o as the tuple (s, D, N_o, E_o), as defined in Section II. To simplify our analysis, we transform G into a complete k-ary tree $G' = (N, E, r)$ on which o is constructed, where N and E are the same as in G, and $r \in N$ is designated as the root router. s is the only host connected to r. Other hosts are connected to routers with equal probability in both G and G' to obtain D. The height of G' is h. To transform G into G', any cycle in G is broken by eliminating the edge on the cycle which no overlay link in o traverses. Such an edge typically exists when the overlay cost is minimized, which is the overlay we consider here, as given in Definition 1 below. In addition, we move the children of nodes whose degree is larger than k, along with the subtrees rooted at these nodes, to nodes which have degree less than k. Such nodes are guaranteed to exist, e.g., leaf nodes. This simple transformation shows that we do not significantly lose generality by considering an underlying tree. The overlay cost exhibited with an underlying tree has also been shown to be more consistent with that exhibited with real topologies, compared to meshes or random graphs [30]. We are, however, currently investigating the average costs for the set of trees covering a power-law and small-world underlying network.

To incorporate the number-of-hops distribution properties discussed in Section III, routers with only one child (and no hosts to be connected) are added between branching points in the underlying network model. Such routers are called *unary nodes*. We had observed that the number of hops between parent and child hosts approximately decreases, as the level of the host in the overlay tree increases. A similar modeling assumption to that in [15] (a *self-similar tree*) can be used to represent this observation. This entails that $A_i = \phi A_{i-1}$, $0 \leq \phi \leq 1$, where A_i is the number of concatenated links generated by unary nodes between a node at level $i-1$ and a node at level i in the underlying network (the notions of levels and h do not consider unary nodes, which are counted separately). Therefore, $k^{(h-i)\theta} - 1$ unary nodes are created between adjacent nodes at levels $i-1$ and i, where $0 \leq \theta < 1$. This implies that $k^{(h-i)\theta}$ links exist at level i from a branching node at level $i-1$. The tree has no unary nodes when $\theta = 0$. Note that the number of hops on overlay links will not be monotonically decreasing (but will be approximately decreasing) for increasing levels of the overlay tree, since data may be disseminated up G' in certain segments, as discussed in the next 2 sections.

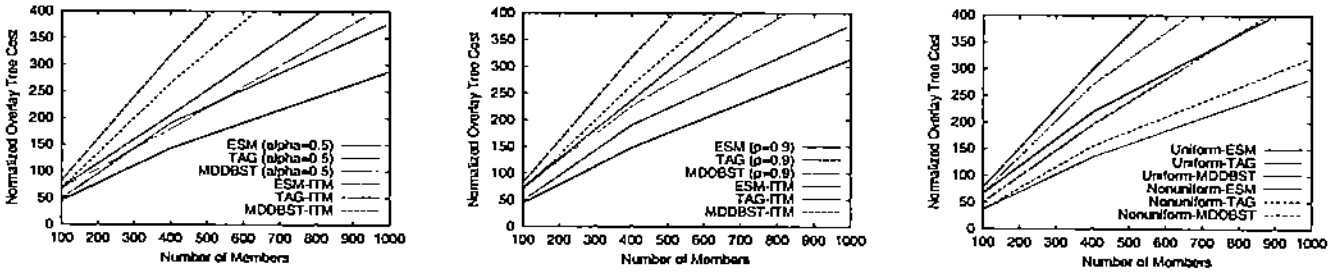

(a) ($\alpha = 0.5, p = 0.5$) versus GT-ITM

(b) ($\alpha = 1.22, p = 0.9$) versus GT-ITM

(c) Uniform versus non-uniform host distributions

Fig. 18. Comparisons of normalized overlay cost for different topologies and host distributions

We assume that each receiver is connected to a router in the network uniformly and independently of other receivers. We use the term $L_o(h,k,n)$ to denote overlay cost for an overlay tree o and number of hosts $|H_o| = n$ (h and k are defined above). In [13], m, the number of distinct routers to which hosts are connected, is used instead of n in $L_o(h,k,n)$. We, however, believe that using the number of hosts n is intuitively appealing and makes analysis simpler. Note that m can be approximated by $M(1-(1-\frac{1}{M})^n)$, where M is the total number of available routers to which hosts can be connected. Therefore, $m \approx n$ when $\frac{n}{M} \ll 1$ [15].

Among all possible overlay networks that can be superimposed on G', we compute the *least cost* overlay network defined as follows.

Definition 1: Let Ω be the set of all possible overlays, connecting a particular set of n hosts, and superimposed on a network G'. Let $L_\tau(h,k,n)$ be the overlay cost for $\tau \in \Omega$. Let o be the least cost overlay on G'. Then, o is the overlay that satisfies $L_o(h,k,n) \leq L_\tau(h,k,n)$ for all $\tau \in \Omega$.

We consider the least cost overlay network for three primary reasons. First, modeling and analysis are simplified in this case. Second, many overlay multicast protocols optimize a delay-related metric, which is typically also optimized by underlying (especially intra-domain) routing protocols. Third, it gives a lower bound on the overlay tree cost under our assumptions.

B. Receivers at Leaf Nodes

We first consider a network in which receivers can only be connected to leaf nodes in the underlying network. Figure 20(a) shows a model of such a network. One host, which is the current source of the overlay multicast session, is connected to the root r of the tree. All other hosts are connected to leaf nodes, selected independently and uniformly. We define ρ to be the lowest level with branching nodes above or at *half* of the tree height. Since $\sum_{i=\rho+1}^{h} k^{(h-i)\theta}$ indicates the height from ρ to the lowest tree level, ρ can be computed as:

$$2\sum_{i=\rho+1}^{h} k^{(h-i)\theta} \leq \sum_{i=1}^{h} k^{(h-i)\theta} \tag{1}$$

Thus,

$$\rho = \left\lceil h - \frac{1}{\theta}\log_k \frac{k^{h\theta}+1}{2} \right\rceil \tag{2}$$

For ease of counting, we first consider a tree without unary nodes and then add the cost introduced by unary nodes. Figure 20(a) shows that the cost incurred when communicating from a receiver to another receiver, both connected to descendants of node σ at level $\lceil \frac{h}{2} \rceil$, is bounded by h. Otherwise, the source would send another copy directly to the receiver at cost h. For this reason, we group together all receivers connected to descendants of σ in a subtree rooted at σ. Similar subtrees are created for every node at level $\lceil \frac{h}{2} \rceil$.

We divide the computation of $L_o(h,k,n)$ into two terms. The first term is the minimum cost to send to the subtrees rooted at σ, and the second term is the minimum cost of data dissemination within the subtrees. To compute the first term, we observe that there are k^ρ nodes at level ρ in the tree. The probability that a link connecting to level ρ is traversed by overlay o is $1-(1-k^{-\rho})^n$. Thus, the cost at level ρ is $k^\rho(1-(1-k^{-\rho})^n)$. Since $k^{(h-i)\theta}$ additional cost is incurred by a node at level i if the tree is extended with *unary nodes*, the first term becomes:

$$\sum_{i=1}^{h} k^{(h-i)\theta} k^\rho (1-(1-k^{-\rho})^n) = \frac{k^{h\theta}-1}{k^\theta - 1} k^\rho (1-(1-k^{-\rho})^n) \tag{3}$$

To compute the second term, we consider a subtree rooted at σ. This subtree and potential overlay links are shown in Figure 20(b). Consider a node α_l at level l, where $\frac{h}{2} \leq l < h$ in the subtree. Let α_{l+1}^0 and α_{l+1}^1 be two children of α_l at level $l+1$. Suppose that A is a receiver connected to a descendant of α_{l+1}^0, and B is a receiver connected to a descendant of α_{l+1}^1. Since $\sum_{i=l+1}^{h} k^{(h-i)\theta} \approx k^{(h-l-1)\theta}$ is incurred due to *unary*

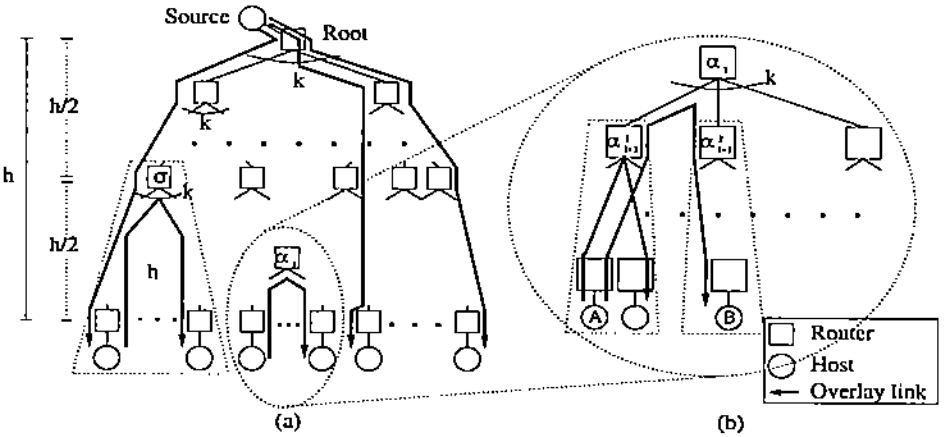

Fig. 20. An overlay tree model with receivers located only at leaf nodes (for simplicity, unary nodes are not shown)

nodes, sending data from A to B across (up and then down) α_l costs:

$$2k^{(h-l-1)\theta} \tag{4}$$

Since there are k^{l+1} links to level $l+1$ of the tree, the probability that a particular link to level $l+1$ is used in o is $1-(1-k^{-(l+1)})^n$. Since α_l has k children, the cost from α_l to its children in o becomes $k(1-(1-k^{-(l+1)})^n)$. An overlay link is created between a pair of children of α_l, so the cost across α_l is $k(1-(1-k^{-(l+1)})^n)-1$. Applying Equation (4) for α_l, the cost at level l in the subtree becomes $2k^{(h-l-1)\theta}(k(1-(1-k^{-(l+1)})^n)-1)$. We, however, note that there must be no link across α_l if the cost from α_l to its children is less than one, that is, $k(1-(1-k^{-(l+1)})^n)<1 \Leftrightarrow l > \ln_k(1-(1-\frac{1}{k})^{\frac{1}{n}})^{-1}-1$. Therefore, the cost at level l in the subtree $g(l)$ is defined as:

$$g(l) = 2k^{(h-l-1)\theta}(k(1-(1-k^{-(l+1)})^n)-1) \tag{5}$$

where $\rho \le l \le \ln_k(1-(1-\frac{1}{k})^{\frac{1}{n}})^{-1}-1$. $g(l)=0$ otherwise. Consequently, the second term becomes:

$$\sum_{l=\rho}^{h-1} k^l g(l) \tag{6}$$

$L_o(h,k,n)$ is the sum of (3) and (6):

$$L_o(h,k,n) = \frac{k^{h\theta}-1}{k^\theta-1}k^\rho(1-(1-k^{-\rho})^n) + \sum_{l=\rho}^{h-1} k^l g(l) \tag{7}$$

We prove that this tree is indeed the least cost overlay tree on this underlying network in the Appendix (Lemma 2). Since the average number of hops on the source to receiver unicast paths $U_o^\theta(h)$ is $\sum_{i=1}^{h} k^{(h-i)\theta} = \frac{k^{h\theta}-1}{k^\theta-1}$, the normalized overlay cost becomes:

$$R_o^\theta(h,k,n) = \frac{L_o(h,k,n)}{U_o^\theta(h)} \tag{8}$$

A power-law is observed in (8), where the exponent of n is $1-\theta$ (see Lemma 3 in the Appendix for details). Figure 21(a) depicts the normalized overlay cost $R_o^\theta(h,k,n)$ against the number of overlay group members n. Note that the total number of routers including unary routers is 356 for $(k=4,h=4)$, 309,819 for $(k=8,h=6)$, 4.6 billion for $(k=16,h=8)$ and more than 4.6 billion for $(k=32,h=10)$. The figure shows that $R_o^\theta(h,k,n) \propto n^{0.92}$, for $0<a<1$. Saturation occurs as $a \to \infty$ $(n \to \infty)$.

C. Receivers at Leaf or Non-leaf Nodes

We now relax the restriction that receivers are only connected to leaf nodes in the underlying network, as illustrated in Figure 22. A non-leaf node with receiver(s) connected receives data from an ancestor, and relays this data to its descendants. In contrast, descendants of a non-leaf node which has no receivers connected must receive data from other non-ancestor nodes.

We use the same underlying network model as in Section IV-B. We now assume that receivers are uniformly and independently distributed over the entire tree (with the exception of unary nodes). This implies that the probability that a node (other than the root) has at least one receiver connected is:

$$p = 1-(1-\frac{1}{M})^n \tag{9}$$

for n receivers, where

$$M = k+\cdots+k^h = \frac{k^{h+1}-k}{k-1} \tag{10}$$

On the average, among the k children of a non-leaf node, kp children have receivers connected, while $k(1-p)$ children have no receivers connected. Let $L_\nu(h,k,n)$ be the overlay cost of an overlay network ν. The computation of $L_\nu(h,k,n)$ is split into two components: (i) cost for kp children of the root with receivers, and (ii) cost for $k(1-p)$ children of the root without receivers. Again, we first consider a tree without unary nodes and then add the cost introduced by unary nodes.

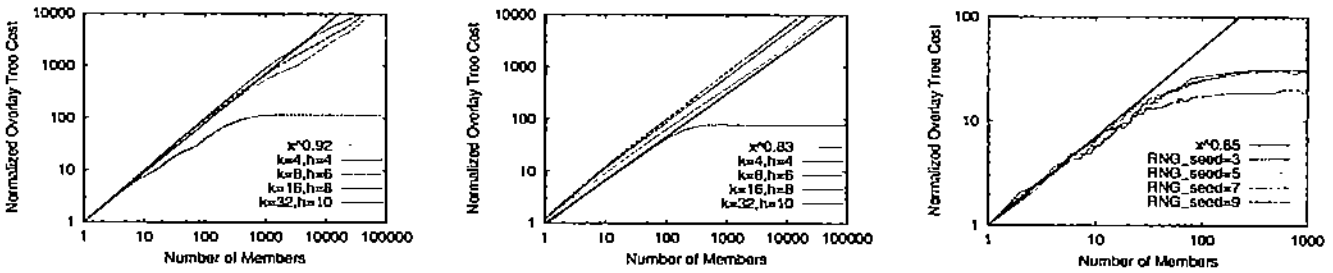

(a) Receivers at leaf nodes

(b) Receivers at leaf or non-leaf nodes

(c) Traceroute-based overlay multicast simulations using minimum spanning trees

Fig. 21. Normalized overlay cost versus number of members from $R_o(h,k,n)$ for (a) and from $R_\nu(h,k,n)$ for (b) ($\theta = 0.1$) and from simulations for (c) (log-log scale)

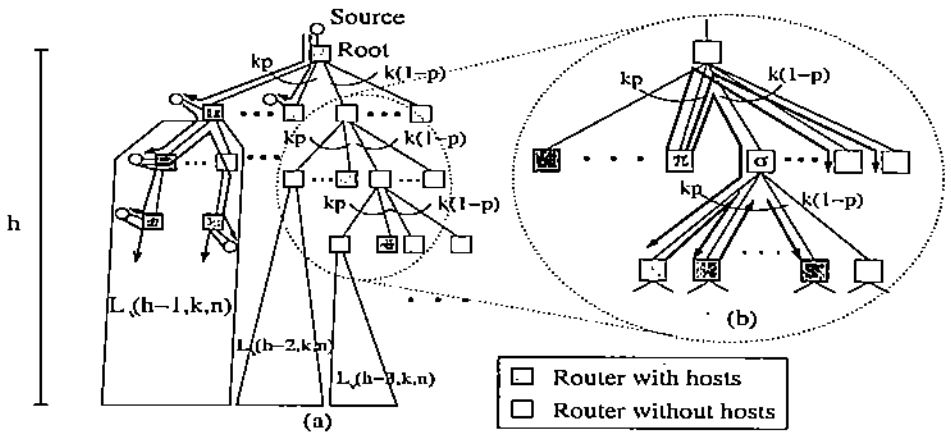

Fig. 22. An overlay tree model with receivers located at leaf or non-leaf nodes (for simplicity, unary nodes are not shown)

In the first component, one of the kp children incurs $k^{(h-1)\theta}$ from the root and $L_\nu(h-1,k,n)$ for its descendants. Thus, the cost for the kp children of the root is:

$$kp(k^{(h-1)\theta} + L_\nu(h-1,k,n)) \tag{11}$$

Now, consider one of the $k(1-p)$ children of the root without receivers. We again have kp children with connected receivers, and $k(1-p)$ children without connected receivers. A recurrence relation based on this pattern computes the second part of $L_\nu(h,k,n)$ for the $k(1-p)$ children of the root. Consider node σ at level l which does not have receivers connected (refer to Figure 22). There may be receivers at the descendants of σ that use the link from the parent of σ to σ with approximate probability:

$$1 - \left(1 - k^{-l}\frac{k^h - k^l}{k^{h+1} - k}\right)^n \tag{12}$$

where k^{-l} is the probability that a receiver is located below σ, and $\frac{k^h - k^l}{k^{h+1} - k}$ is the probability that the receiver is connected to a non-leaf node at level i, $l < i < h$. The latter probability is based on the fact that the total number of nodes except the root is $k + \cdots + k^h = \frac{k^{h+1}-k}{k-1}$ and the number of nodes at level i is $\frac{k^h - k^l}{k-1}$. We use $1-(1-k^{-l})^n$ as an approximation of Equation (12) for large h values.

Let $T(l)$ denote the cost required to deliver data to the descendants of σ. As illustrated in Figure 22, at least one of the kp children must receive data from nodes other than σ and the descendants of σ. If we consider the additional cost introduced by *unary nodes*, a sibling node of σ which has receivers (π in the figure) minimizes the cost to $2k^{(h-l)\theta} + k^{(h-l-1)\theta}$. An additional cost of $2k^{(h-l-1)\theta}(kp-1)$ is required to relay the data among the kp children of σ. Thus, $B(h-l-1) = k^{(h-l-1)\theta}(2k^\theta + 2kp - 1)(1-(1-k^{-l})^n)$ is incurred for the kp children of σ. Also, $kpL_\nu(h-l-1,k,n)$ is incurred by the descendants of the kp children of σ. For the $k(1-p)$ children of σ without receivers, $k(1-p)T(l+1)$ is incurred. Hence, $T(l)$ can be computed as:

$$\begin{aligned} T(l) &= B(h-l-1) \\ &\quad + kpL_\nu(h-l-1,k,n) + k(1-p)T(l+1) \\ &= \sum_{i=l}^{h-1} k^{i-l}(1-p)^{i-l} \\ &\quad \times \{B(h-i-1) + kpL_\nu(h-i-1,k,n)\} \end{aligned} \tag{13}$$

The cost for the $k(1-p)$ children of the root at level $l=1$ is:

$$k(1-p)T(l=1) = \sum_{i=1}^{h-1} k^i(1-p)^i \times\{B(h-i-1) + kpL_\nu(h-i-1,k,n)\} \quad (14)$$

Therefore,

$$L_\nu(h,k,n) = kp(k^{(h-1)\theta} + L_\nu(h-1,k,n)) + \sum_{i=1}^{h-1} k^i(1-p)^i\{B(h-i-1) + kpL_\nu(h-i-1,k,n)\} \quad (15)$$

Lemma 1: Solving the recurrence relation in Equation (15) with a fixed ratio $a = \frac{n}{M}$ $(0 < a < \infty)$ (M is as defined in Equation (10)) yields:

$$L_\nu(h,k,n) = k^{(h-1)\theta+1}p + (k^h + k^{h\theta}\sum_{i=2}^{h-1} k^{(1-\theta)i})p^2 + k^{(h-2)\theta+1}(1-p)(2k^\theta + 2kp - 1)\sum_{i=0}^{h-2} k^{(1-\theta)i} - k^{h-\theta}(1-p)(2k^\theta + 2kp - 1)c_2(a,\theta) + O(1) \quad (16)$$

where

$$c_2(a,\theta) = \sum_{i=0}^{\infty} k^{-(1-\theta)i} e^{-ak^{i+1}} \quad (17)$$

The proof of Lemma 1 and the proof that $L_\nu(h,k,n)$ is the minimum cost overlay tree when receivers are located at any node except the root (Lemma 4) can be found in the Appendix. Note that $U_\nu^\theta(h,k)$, the average number of hops on the source to receiver unicast paths, is now computed as:

$$U_\nu^\theta(h,k) = \frac{1}{M}\sum_{l=1}^{h} k^l \sum_{i=1}^{l} k^{(h-i)\theta} \quad (18)$$

The normalized overlay cost $R_\nu^\theta(h,k,n) = \frac{L_\nu(h,k,n)}{U_\nu^\theta(h,k)}$ does not exhibit a power-law (see Lemma 5 in the Appendix). However, Figure 21(b) demonstrates that $R_\nu^\theta(h,k,n)$ behaves asymptotically similar to a power-law when $0 < a < 1$. The total numbers of routers is the same as in Figure 21(a). In the figure, $R_\nu^\theta(h,k,n) \propto n^{0.83}$. The factor 0.83 is *smaller* than the 0.92 for the case when hosts are only connected at leaves, since many additional hops can be saved in this case. It is also important to note that our decreasing unary node distribution leads to a lower tree cost (0.83 versus an 0.87 factor for this same model with uniformly distributed unary nodes). The cost provides a useful notion for comparing and designing overlay multicast protocols to optimize loads. The 0.8 to 0.9 factor can be also compared to a factor ≈ 0.7 for IP multicast [12], [13].

D. Simulation and Experimental Validation

We validate our analytical results using a traceroute-based simulation topology. (Our methodology for synthesizing the routes is discussed in Section III-A.) We simulate hosts connected to edge routers by randomly connecting 1000 hosts to the edge routers connected to 60 selected traceroute servers. The total number of routers including unary routers is approximately 18,957. We first construct an overlay that is a complete graph among these 1000 hosts. In order to be consistent with our modeling assumption that the least cost overlay tree is used, we compute the minimum spanning tree on that graph. An important difference, however, is that a host in the overlay tree enforces an upper degree bound (UDB) on the maximum number of children, to simulate bandwidth constraints. (Hosts connected to the same router are not considered in the UDB check.)

Figure 21(c) shows the normalized overlay cost versus the number of members with UDB=6. Four different random number generator seeds (RNG_seed=3,5,7,9) are used for the assignment of hosts. We observe that the results are consistent with our modeling results. The normalized overlay cost is asymptotically close to $n^{0.85}$ or so, for a small number of members (< 100). The value was higher ($n^{0.87}$) when we repeated the same experiment with UDB=1. The tree cost saturates at around 36, when the number of members is ≈ 100, which is earlier than the curves in Figure 21(b). This can be attributed to the usage of only 60 routers to which hosts are connected in the simulation, versus a much larger number of routers used in Figure 21(b).

We have also examined the normalized overlay cost via simulations of the three overlay protocols on the topologies described in Section III-B. The results reveal that ESM and MDDBST behave asymptotically close to $n^{0.8} - n^{0.9}$ or so, before they saturate, which is consistent with our analytical results. TAG has a slightly higher cost than ESM and MDDBST. Partial path matching in TAG may incur higher costs due to the u unmatched routers allowed with high *bwthresh* values. We also found that the normalized cost was higher for the GT-ITM topologies than for the power-law and small-world topologies, since router degree and clustering properties are exploited by overlay protocols to reduce stress and cost.

To further validate our results, we compute the stress and overlay cost for the real ESM tree used in Section III-A. We find that the maximum stress is 12, the total stress is 696, and the overlay tree cost is 568. Since the average unicast path length is ≈ 12.01, the normalized overlay cost is $\frac{568}{12.01} \approx 47.3$. Since $n = 59$ (we only use hosts for which we could obtain underlying routes), the normalized tree cost $\approx n^{0.945}$.

V. Related Work

Our objectives in this paper overlap with the objectives of work evaluating IP multicast efficiency. Chuang and Sirbu [13] were first to investigate the efficiency of IP multicast in terms of network traffic load. They found that the

ratio between the total number of multicast links and the average unicast path length exhibits a power-law with respect to the number of distinct sites with multicast receivers ($m^{0.8}$). Their conclusion was based on real and generated network topologies. Chalmers and Almeroth [12] subsequently investigated the efficiency of IP multicast over unicast experimentally. They carefully analyzed numerous real and synthetic Internet data sets. They argue that the normalized tree cost is closer to $n^{0.7}$ than to $n^{0.8}$. In addition, their results indicate that multicast trees typically include a high frequency (70 to 80%) of unary nodes.

In order to precisely understand the causes of IP multicast traffic reduction, several mathematical models have been devised. Phillips *et al.* [14] were first to derive asymptotic forms for the power-law in k-ary trees and more general networks. Their models, however, are approximate and cannot precisely explain the 0.8 (or 0.7) power-law. Adjih *et al.* [15] obtained more accurate asymptotic forms of the power-law. They show that the essence of the problem is the modeling assumption. To prove this, the simple k-ary tree used in [14] is abandoned, and a k-ary *self-similar* tree is used. The authors argue that the self-similar tree provides a plausible explanation of the power-law. However, no experimental data is provided to prove that IP multicast trees are indeed self-similar, i.e., the number of unary nodes decreases as the tree level increases. Mieghem *et al.* [31] have also analyzed the Chuang and Sirbu result. The expected number of joint hops in a shortest-path multicast tree is used to compute the expected number of links.

We consider the case of overlay multicast, not IP multicast, in this paper. A number of overlay multicast protocols have been proposed over the last three years. ESM (or Narada) [1], [16] was one of the earliest approaches. ESM hosts exchange group membership and routing information to build a mesh, and then execute a DVMRP-like protocol to construct a forwarding tree. ESM first considers bandwidth, then latency. A hierarchical approach to improve scalability is proposed in [3]. CAN-based multicast [28] partitions members into bins using proximity information obtained from DNS and delay measurements. In [5], the authors utilize host degree constraints and diameter bounds to centrally compute an optimal overlay multicast network. TAG [4] uses route overlap as a heuristic for constructing a low-delay overlay tree in a distributed manner. Graph-theoretic models are used in [29] to explore hybrid proxy and overlay multicast trees with delay and bandwidth bounds. Recently, flooding-based and tree-based overlay multicast on CAN [10] and Pastry [11] were compared in [32].

Perhaps the work that comes closest to ours is presented in [30] and [25]. Radoslavov *et al.* [30] characterized real and generated topologies with respect to neighborhood size growth, robustness, and increase in path lengths due to link failure. They briefly analyzed the impact of topology on two heuristic overlay multicast strategies, in terms of stretch (the ratio of the number of links in overlay multicast to that in IP multicast) and maximum link stress. Jin and Bestavros [25] have shown that both Internet AS-level and router-level graphs exhibit small-world behavior, due to power-law degree distributions and preference to local connections. They also outlined how small-world behavior affects the overlay multicast tree size.

VI. Conclusions and Future Work

We have characterized overlay multicast trees via experimental data and simulations of three overlay multicast protocols. We also have modeled and computed the overlay cost, defined as the total number of hops in all overlay links. Based on our results, we can make the following observations. First, the experimental data and simulations illustrate that both the average delay and the number of hops between parent and child hosts tend to decrease as the level of the host in the overlay tree increases. Our analysis suggests that routing features in overlay multicast protocols, along with power-law and small-world topology characteristics, play a key role in explaining these phenomena. Non-uniform multicast host distribution reinforces them. Second, our models behave asymptotically close to power-laws, ranging from $n^{0.83}$ to $n^{0.92}$ for n hosts. Simulations and experimental data validate our models, and show the latency bandwidth tradeoffs in overlay trees constructed via three different protocols. We can quantify potential bandwidth savings of overlay multicast compared to unicast since $n^{0.9} < n$, and the bandwidth penalty of overlay multicast compared to IP multicast ($n^{0.9} > n^{0.8}$).

One limitation of our experiments is the synthesis of traceroute paths among hosts. Topology inference projects [33] may help us obtain more accurate path information for our future experiments and analysis. We plan to conduct larger-scale simulations and experimental data analysis to better understand overlay tree properties. We will also examine other types overlay protocols, and investigate more dynamic characteristics and performance metrics, including join-leave dynamics, protocol overhead, and delay and bandwidth changes. Finally, we plan to precisely formulate the relationship between the structure of overlay trees, overlay protocols, and Internet topology characteristics. This will ultimately shed more light on overlay protocol design methodologies.

References

[1] Y. Chu, S. Rao, S. Seshan, and H. Zhang, "Enabling Conferencing Applications on the Internet using an Overlay Multicast Architecture," in *Proc. of ACM SIGCOMM*, August 2001, pp. 55–67.

[2] J. Jannotti, D. Gifford, K. Johnson, M. Kaashoek, and J. OToole Jr., "Overcast: Reliable multicasting with an overlay network," in *Proc. of OSDI*, October 2000.

[3] S. Banerjee, B. Bhattacharjee, and C. Kommareddy, "Scalable Application Multicast," in *Proc. of ACM SIGCOMM*, August 2002.

[4] M. Kwon and S. Fahmy, "Topology-Aware Overlay Networks for Group Communication," in *Proc. of ACM NOSSDAV*, May 2002, pp. 127–136.

[5] S. Shi, J. Turner, and M. Waldvogel, "Dimensioning server access bandwidth and multicast routing in overlay networks," in *Proc. of ACM NOSSDAV*, June 2001, pp. 83–91.

[6] S. Savage, T. Anderson, A. Aggarwal, D. Becker, N. Cardwell, A. Collins, E. Hoffman, J. Snell, A. Vahdat, G. Voelker, and J. Zahorjan, "Detour: a Case for Informed Internet Routing and Transport," *IEEE Micro*, vol. 1, no. 19, pp. 50–59, January 1999.

[7] David G. Andersen, Hari Balakrishnan, M. Frans Kaashoek, and Robert

Morris, "Resilient Overlay Networks," in *Proc. of ACM SOSP*, October 2001, pp. 131–145.
[8] J. Byers, J. Considine, M. Mitzenmacher, and S. Rost, "Informed Content Delivery Across Adaptive Overlay Networks," in *Proc. of ACM SIGCOMM*, August 2002.
[9] I. Stoica, R. Morris, D. Liben-Nowell, D. R. Karger, M. F. Kaashoek, F. Dabek, and H. Balakrishnan, "Chord: A Scalable Peer-to-peer Lookup Protocol for Internet Applications," in *Proc. of ACM SIGCOMM*, August 2001, pp. 149–160.
[10] S. Ratnasamy, P. Francis, M. Handley, R. Karp, and S. Shenker, "A Scalable Content-Addressable Network," in *Proc. of ACM SIGCOMM*, August 2001, pp. 161–172.
[11] A. Rowstron and P. Druschel, "Pastry: Scalable, Decentralized Object Location and Routing for Large-scale Peer-to-Peer Systems," in *Proc. of ACM/IFIP Middleware*, 2001.
[12] R. Chalmers and K. Almeroth, "Modeling the Branching Characteristics and Efficiency Gains in Global Multicast Trees," in *Proc. of IEEE INFOCOM*, April 2001, pp. 449–458.
[13] J. Chuang and M. Sirbu, "Pricing Multicast Communications: A Cost-Based Approach," in *Proc. of Internet Society INET*, July 1998.
[14] G. Phillips, S. Shenker, and H. Tangmunarunkit, "Scaling of Multicast Trees: Comments on the Chuang-Sirbu scaling law," in *Proc. of ACM SIGCOMM*, 1999, pp. 41–51.
[15] C. Adjih, L. Georgiadis, P. Jacquet, and W. Szpankowski, "Multicast Tree Structure and the Power Law," in *Proc. of SODA*, 2002.
[16] Y. Chu, S. Rao, and H. Zhang, "A Case for End System Multicast," in *Proc. of ACM SIGMETRICS*, June 2000, pp. 1–12.
[17] "Traceroute.org," 2003, http://www.traceroute.org.
[18] D. V. Houweling, "Internet 2," 2003, http://www.internet2.edu.
[19] M. Faloutsos, P. Faloutsos, and C. Faloutsos, "On Power-Law Relationships of the Internet Topology," in *Proc. of ACM SIGCOMM*, August 1999, pp. 251–262.
[20] D. Watts and S. Strogatz, "Collective Dynamics of Small-world Networks," *Nature*, vol. 363, pp. 202–204, 1998.
[21] A. Barabasi and R. Albert, "Emergence of Scaling in Random Networks," *Science*, vol. 286, pp. 509–512, 1999.
[22] L. Peterson, T. Anderson, D. Culler, and T. Roscoe, "A Blueprint for Introducing Disruptive Technology into the Internet," in *Proceedings of the HotNets-I*, October 2002.
[23] A. Kuznetsov, "Tracepath," ftp://ftp.inr.ac.ru/ip-routing/iputils-current.tar.gz.
[24] J. Winick and S. Jamin, "Inet-3.0: Internet Topology Generator," Tech. Rep. UM-CSE-TR-456-02, Univ. of Michigan, 2002.
[25] S. Jin and A. Bestavros, "Small-World Internet Topologies: Possible Causes and Implications on Scalability of End-System Multicast," Tech. Rep. BUCS-TR-2002-004, Boston University, 2002.
[26] E. Zegura, K. Calvert, and S. Bhattacharjee, "How to Model an Internetwork," in *Proc. of IEEE INFOCOM*, March 1996, vol. 2, pp. 594–602.
[27] M. Castro, P. Druschel, A.-M. Kermarrec, and A. Rowstron, "Scribe: A Large-scale and Decentralized Application-level Multicast Infrastructure," *IEEE Journal on Selected Areas in Communications*, vol. 20, no. 8, October 2002.
[28] S. Ratnasamy, M. Handley, R. Karp, and S. Shenker, "Topologically-Aware Overlay Construction and Server Selection," in *Proc. of IEEE INFOCOM*, June 2002, vol. 3, pp. 1190–1199.
[29] N. Malouch, Z. Liu, D. Rubenstein, and S. Sahu, "A Graph Theoretic Approach to Bounding Delay in Proxy-Assisted, End-System Multicast," in *Proc. of IWQoS*, May 2002.
[30] P. Radoslavov, H. Tangmunarunkit, H. Yu, R. Govindan, S. Shenker, and D. Estrin, "On Characterizing Network Topologies and Analyzing Their Impact on Protocol Design," Tech. Rep. USC-CS-TR-00-731, Dept. of Computer Science, University of Southern California, February 2000.
[31] P. Mieghem, G. Hooghiemstra, and R. Hofstad, "On the Efficiency of Multicast," *IEEE/ACM Transactions on Networking*, vol. 9, no. 6, December 2001.
[32] M. Castro, M. B. Jones, A-M. Kermarrec, A. Rowstron, M. Theimer, H. Wang, and A. Wolman, "An Evaluation of Scalable Application-level Multicast Built Using Peer-to-peer Overlays," in *Proc. of IEEE INFOCOM*, March-April 2003.
[33] P. Francis, S. Jamin, C. Jin, Y. Jin, D. Raz, Y. Shavitt, and L. Zhang, "IDMaps: A Global Internet Host Distance Estimation Service," *IEEE/ACM Transactions on Networking*, vol. 9, no. 5, pp. 525–540, October 2001.
[34] W. Szpankowski, *Average Case Analysis of Algorithms in Sequences*, John Wiley & Sons, New York, 2001.

APPENDIX

Proof of Lemma 1

Since $L_\nu(h-1,k,n)$ is

$$L_\nu(h-1,k,n) = kp(k^{(h-2)\theta} + L_\nu(h-2,k,n)) + \sum_{i=1}^{h-2} k^i(1-p)^i\{B(h-i-2) + kpL_\nu(h-i-2,k,n)\} \quad (19)$$

$L_\nu(h,k,n)$ becomes

$$\begin{aligned}
L_\nu(h,k,n) &= kp(k^{(h-1)\theta} + L_\nu(h-1,k,n)) \\
&+ \sum_{i=1}^{h-1} k^i(1-p)^i\{B(h-i-1) + kpL_\nu(h-i-1,k,n)\} \\
&= k^{(h-1)\theta+1}p + k^2p^2(k^{(h-2)\theta} + L_\nu(h-2,k,n)) \\
&+ kp\sum_{i=1}^{h-2} k^i(1-p)^i\{B(h-i-2) \\
&+ kpL_\nu(h-i-2,k,n)\} \\
&+ \sum_{i=1}^{h-1} k^i(1-p)^i\{B(h-i-1) + kpL_\nu(h-i-1,k,n)\} \\
&= k^{(h-1)\theta+1}p + k^2p^2k^{(h-2)\theta} + k^2pL_\nu(h-2,k,n) \\
&+ \sum_{i=2}^{h-1} k^i(1-p)^{i-1}\{B(h-i-1) \\
&+ kpL_\nu(h-i-1,k,n)\} + k(1-p)B(h-2) \quad (20) \\
&= k^{(h-1)\theta+1}p + p^2(k^2k^{(h-2)\theta} + k^3k^{(h-3)\theta}) \\
&+ k^3pL_\nu(h-3,k,n) + \sum_{i=3}^{h-1} k^i(1-p)^{i-2}\{B(h-i-1) \\
&+ kpL_\nu(h-i-1,k,n)\} + k(1-p)(B(h-2) + kB(h-3))
\end{aligned}$$

where

$$B(h-i-1) = k^{(h-i-1)\theta}(2k^\theta + 2kp - 1)(1-(1-k^{-i})^n) \quad (21)$$

Repetition of this process finally yields

$$\begin{aligned}
L_\nu(h,k,n) &= k^{(h-1)\theta+1}p + p^2\sum_{i=2}^{h-1} k^ik^{(h-i)\theta} \quad (22) \\
&+ k^{h-1}pL_\nu(1,k,n) + k^{h-1}(1-p)B(0) \\
&+ k(1-p)\sum_{i=0}^{h-3} k^iB(h-i-2) \\
&= k^{(h-1)\theta+1}p + k^{h\theta}p^2\sum_{i=2}^{h-1} k^{(1-\theta)i} + k^hp^2 \\
&+ k^{(h-2)\theta+1}(1-p)(2k^\theta + 2kp - 1)\sum_{i=0}^{h-2} k^{(1-\theta)i}
\end{aligned}$$

$$-k^{(h-2)\theta+1}(1-p)(2k^\theta+2kp-1)\sum_{i=1}^{h-1}k^{(1-\theta)i}(1-k^{-i})^n$$

where $L_\nu(1,k,n)=kp$ and $L_\nu(0,k,n)=0$. By $j=h-1-i$, we have

$$\sum_{i=1}^{h-1}k^{(1-\theta)i}(1-k^{-i})^n = k^{(1-\theta)(h-1)}\sum_{j=0}^{h-2}k^{-(1-\theta)j}\left(1-\frac{k^j}{k^{h-1}}\right)^n \quad (23)$$

As analyzed in the Appendix A.1 of [15],

$$\sum_{j=0}^{h-2}k^{-(1-\theta)j}\left(1-\frac{k^j}{k^{h-1}}\right)^n = c_2(a,\theta)+O(1) \quad (24)$$

where

$$c_2(a,\theta)=\sum_{i=0}^{\infty}k^{-(1-\theta)i}e^{-ak^{i+1}} \quad (25)$$

Thus,

$$\sum_{i=1}^{h-1}k^{-(1-\theta)i}(1-k^{-i})^n = k^{(1-\theta)(h-1)}c_2(a,\theta)+O(1) \quad (26)$$

Finally,

$$\begin{aligned}L_\nu(h,k,n) &= k^{(h-1)\theta+1}p+(k^h+k^{h\theta}\sum_{i=2}^{h-1}k^{(1-\theta)i})p^2\\ &+k^{(h-2)\theta+1}(1-p)(2k^\theta+2kp-1)\sum_{i=0}^{h-2}k^{(1-\theta)i}\\ &-k^{h-\theta}(1-p)(2k^\theta+2kp-1)c_2(a,\theta)+O(1) \quad (27)\end{aligned}$$

■

Lemma 2: o is the least cost overlay network when receivers can only be connected to leaf nodes.

Proof: Every receiver except the source in an overlay multicast network needs a parent that sends data. Consider receivers in the subtree rooted at router σ at level $\frac{\xi}{2}$ in a k-ary tree with unary nodes defined in Section IV-B, where $\xi=\sum_{i=1}^{h}k^{(h-i)\theta}$. Communication between two receivers in the subtree consumes at most ξ underlying links (when the communication occurs across σ). In contrast, the number of links from the source to a receiver in the subtree is ξ, and the number of links from a receiver outside the subtree to a receiver in the subtree is at least $2(\frac{\xi}{2}+1)=\xi+2$. Hence, the number of links between two receivers in the subtree is no larger than the number of links from a host outside the subtree to a receiver in the subtree. Therefore, receivers in the subtree should have their parents in the same subtree to minimize the number of links. However, at least one receiver in the subtree must receive data from a host outside the subtree. Sending data from the source to a receiver minimizes this communication to ξ links. The minimal number of links between the receivers in the subtree can be computed as follows. Suppose that we compute the least number of links traversed across α_l at level l, where $\frac{\xi}{2}\le l<\xi$ in Figure 20(b). If the subtree rooted at α_{l+1}^2 has at least one receiver such as B, there must be a connection from a receiver outside this subtree to B. In this case, the connection from A to B consumes the least cost, $2(\xi-l)$, in the figure. Similarly, we can compute the smallest number of links in the subtree rooted at σ recursively. ■

Lemma 3: For a fixed ratio $a=\frac{n}{k^h}$, when $0<a<\infty$, $L_o(h,n)$ has the following asymptotic expansions:
(i) When $\ln_k(1-(1-\frac{1}{k})^{\frac{1}{n}})^{-1}-1<\rho$,

$$L_o(h,k,n)=\frac{k^{h\theta}-1}{k^\theta-1}k^\rho(1-(1-k^{-\rho})^n) \quad (28)$$

(ii) Otherwise, that is, when n is large,

$$\begin{aligned}L_o(h,k,n) &= \frac{k^{h\theta}-1}{k^\theta-1}k^\rho+2(k^h-k^{(h-\rho)\theta+\rho})\\ &\times\left(\frac{k-1}{k-k^\theta}-c_1(a,\theta)\right)+O(1) \quad (29)\end{aligned}$$

where

$$c_1(a,\theta)=\sum_{i=0}^{\infty}k^{(-1+\theta)i}e^{-ak^i} \quad (30)$$

Proof: The result in (i) is obtained easily when $g(l)=0$. In (ii), we only need to compute the following.

$$\begin{aligned}&\sum_{l=\rho}^{h-1}k^l g(l)\\ &=2\sum_{l=\rho}^{h-1}k^l k^{(h-l-1)\theta}(k(1-(1-k^{-(l+1)})^n)-1)\\ &=2k^{-\theta}\{\sum_{l=\rho}^{h-1}k^{(h-l)\theta}k^{l+1}(1-(1-k^{-(l+1)})^n)\\ &-\sum_{l=\rho}^{h-1}k^{(h-l)\theta}k^l\} \quad (31)\end{aligned}$$

By $i=l+1$, the first term in (31) is computed as follows.

$$\begin{aligned}&\sum_{l=\rho}^{h-1}k^{(h-l)\theta}k^{l+1}(1-(1-k^{-(l+1)})^n)\\ &=k^\theta\sum_{i=\rho+1}^{h}k^{(h-i)\theta}k^i(1-(1-k^{-i})^n)\\ &=k^\theta\{\sum_{i=1}^{h}k^{(h-i)\theta}k^i(1-(1-k^{-i})^n)\\ &-k^{(h-\rho)\theta}\sum_{i=1}^{\rho}k^{(\rho-i)\theta}k^i(1-(1-k^{-i})^n)\} \quad (32)\end{aligned}$$

This can be rewritten as

$$k^{h+\theta}\left(\frac{k^{1-\theta}}{k^{1-\theta}-1}-c_1(a,\theta)\right) \quad (33)$$

$$-k^{(h-\rho)\theta+\rho+\theta}\left(\frac{k^{1-\theta}}{k^{1-\theta}-1}-c_1(a,\theta)\right)+O(1)$$

using the analysis in Appendix A.1 of [15],

$$\sum_{i=1}^{h} k^{(h-i)\theta}k^i(1-(1-k^{-i})^n = \tag{34}$$
$$k^h\left(\frac{k^{1-\theta}}{k^{1-\theta}-1}-c_1(a,\theta)\right)+O(1)$$

where

$$c_1(a,\theta)=\sum_{i=0}^{\infty}k^{(-1+\theta)i}e^{-ak^i} \tag{35}$$

The second term is

$$\sum_{l=\rho}^{h-1}k^{(h-l)\theta}k^l=\frac{k^{h+\theta}-k^{(h-\rho+1)\theta+\rho}}{k-k^\theta} \tag{36}$$

Now, $\sum_{l=\rho}^{h-1}k^l g(l)$ becomes

$$\sum_{l=\rho}^{h-1}k^l g(l) = 2k^{-\theta}((k^{h+\theta}-k^{(h-\rho)\theta+\rho+\theta})$$
$$\times\left(\frac{k^{1-\theta}}{k^{1-\theta}-1}-c_1(a,\theta)\right)-\frac{k^{h+\theta}-k^{(h-\rho+1)\theta+\rho}}{k-k^\theta})+O(1)$$
$$=2(k^h-k^{(h-\rho)\theta+\rho})\left(\frac{k-1}{k-k^\theta}-c_1(a,\theta)\right)+O(1) \tag{37}$$

From equation (37), when n is large,

$$L_o(h,k,n)=\frac{k^{h\theta}-1}{k^\theta-1}k^\rho \tag{38}$$
$$+2(k^h-k^{(h-\rho)\theta+\rho})\left(\frac{k-1}{k-k^\theta}-c_1(a,\theta)\right)+O(1)$$

■

Corollary 1: Under the same conditions as in Lemma 3 (ii), (i) For $a\to 0$, we have

$$L_o(h,k,n)\approx$$
$$2n^{1-\theta}(k^{h\theta}-k^{(2h-\rho)\theta-h+\rho})\left(\frac{\Gamma(\theta)}{(1-\theta)\ln k}-\psi_1(\ln a)\right)$$
$$+\frac{k^{h\theta}-1}{k^\theta-1}k^\rho-\frac{2(k^h-k^{(h-\rho)\theta+\rho})}{k-k^\theta} \tag{39}$$

where

$$\psi_1(x)=\sum_{k=-\infty,k\neq 0}^{\infty}\frac{\Gamma(-1+\theta-\frac{2\pi ik}{\ln k})}{\ln k}e^{2\pi ik\frac{x}{\ln k}} \tag{40}$$

(ii) For $a\to 1$, $L_o(h,k,n)$ is approximated by

$$L_o(h,k,n)\approx\frac{k^{h\theta}-1}{k^\theta-1}k^\rho+2(k^h-k^{(h-\rho)\theta+\rho}) \tag{41}$$
$$\times\left(\frac{k-1}{k-k^\theta}-C_1(\theta)+C_2(\theta)(a-1)-C_3(\theta)(a-1)^2\right)$$

where

$$C_1(a)=\sum_{i=0}^{\infty}k^{-\theta i}e^{-k^i},\quad C_2(a)=\sum_{i=0}^{\infty}k^{\theta i}e^{-k^i}(a-1),$$
$$C_3(a)=\sum_{i=0}^{\infty}k^{(1+\theta)i}e^{-k^i}(a-1)^2 \tag{42}$$

(iii) For $a\to\infty$, $L_o(h,k,n)$ asymptotically becomes

$$L_o(h,k,n)\approx\frac{k^{h\theta}-1}{k^\theta-1}k^\rho+2(k^h-k^{(h-\rho)\theta+\rho})\left(\frac{k-1}{k-k^\theta}-e^{-a}\right) \tag{43}$$

Proof: By Taylor's expansion, as $a\to\infty$, (ii) and (iii) are easy to compute. We compute (i) when $a\to 0$. Using the Mellin transform [34], $c_1(a,\theta)$ is derived as follows (the details the same as those given in [15]).

$$c_1(a,\theta)=\frac{k^{1-\theta}}{k^{1-\theta}-1}-\frac{a^{1-\theta}\Gamma(\theta)}{(1-\theta)\ln k}+a^{1-\theta}\psi_1(\ln a)+O(1) \tag{44}$$

where

$$\psi_1(x)=\sum_{k=-\infty,k\neq 0}^{\infty}\frac{\Gamma(-1+\theta-\frac{2\pi ik}{\ln k})}{\ln k}e^{2\pi ik\frac{x}{\ln k}} \tag{45}$$

Then $L_o(h,k,n)$ becomes

$$L_o(h,k,n)\approx$$
$$2n^{1-\theta}(k^{h\theta}-k^{(2h-\rho)\theta-h+\rho})\left(\frac{\Gamma(\theta)}{(1-\theta)\ln k}-\psi_1(\ln a)\right)$$
$$+\frac{k^{h\theta}-1}{k^\theta-1}k^\rho-\frac{2(k^h-k^{(h-\rho)\theta+\rho})}{k-k^\theta} \tag{46}$$

Considering that the average number of links for unicast $U_o^\theta(h)$ is $\sum_{i=1}^{h}k^{(h-i)\theta}=\frac{k^{h\theta}-1}{k^\theta-1}$, we gain:

$$R_o^\theta(h,k,n) = \frac{L_o(h,k,n)}{U_o^\theta(h)} \tag{47}$$
$$= n^{1-\theta}\frac{2(k^\theta-1)(k^{h\theta}-k^{(2h-\rho)\theta-h+\rho})}{k^{h\theta}-1}$$
$$\times\left(\frac{\Gamma(\theta)}{(1-\theta)\ln k}-\psi_1(\ln a)\right)$$
$$+k^\rho-\frac{2(k^\theta-1)(k^h-k^{(h-\rho)\theta+\rho})}{(k^{h\theta}-1)(k-k^\theta)}$$

as normalized overlay tree cost for (i) in Corollary 1. ■

Lemma 4: ν is the least cost overlay network when receivers can be connected to either leaf or non-leaf nodes.

Proof: Let x be a child node of the root. Let receiver a be a receiver in subtree X rooted at x in Figure 22. The minimum number of links from a host outside X to host b in X is always larger than or equal to the minimum number of links in the relay from the source to a and to b, because the former

relay should cross the source. Hence, we can minimize the number of links by the latter relay and recursive computing in X. We now consider a node σ without a receiver in the figure. Let y be a child of σ with receivers connected to it, and let Y be the subtree rooted at y. Two links from another child of σ with receivers to y and the least number of links in Y (can be computed recursively) minimize the number of links in this case. At least one receiver at the children of σ, however, must receive data from a host which is not at the children of σ. π in the figure minimizes this communication to three links. Note that this communication uses two links when σ is a child of the root. The smallest number of links in the subtree rooted at a child of σ without a receiver can also be computed recursively. ■

Lemma 5: $L_\nu(h,k,n)$ can be approximated with a fixed ratio $a = \frac{n}{M}$ $(0 < a < \infty)$ for large n and M,

$$\begin{aligned} L_\nu(h,k,n) &= k^{(h-1)\theta+1}(1-e^{-a}) \\ &+(k^h + k^{h\theta}\sum_{i=2}^{h-1} k^{(1-\theta)i})(1-e^{-a})^2 \\ &+k^{(h-2)\theta+1}e^{-a}(2k^\theta + 2k(1-e^{-a}) - 1)\sum_{i=0}^{h-2} k^{(1-\theta)i} \\ &-k^{h-\theta}e^{-a}(2k^\theta + 2k(1-e^{-a}) - 1)c_2(a,\theta) \end{aligned} \quad (48)$$

Proof: The result can be derived by $p = 1-(1-\frac{1}{M})^n \approx 1-e^{-a}$. ■

Corollary 2: Under the same conditions as in Lemma 5,
(i) For $a \to 0$ and $a \to 1$, $L_\nu(h,k,n)$ asymptotically becomes

$$\begin{aligned} L_\nu(h,k,n) &= k^{(h-1)\theta+1}\left(a - \frac{a^2}{2}\right) \\ &+(k^h + k^{h\theta}h_1(\theta))\left(a-\frac{a^2}{2}\right)^2 + k^{(h-2)\theta+1} \\ &\times\left(1-a+\frac{a^2}{2}\right)\left(2k^\theta + 2k\left(a-\frac{a^2}{2}\right)-1\right)h_2(\theta) \\ &-k^{h-\theta}\left(1-a+\frac{a^2}{2}\right)\left(2k^\theta + 2k\left(a-\frac{a^2}{2}\right)-1\right)c_2(a,\theta) \end{aligned} \quad (49)$$

where

$$h_1(\theta) = \sum_{i=2}^{h-1} k^{(1-\theta)i}, \quad h_2(\theta) = \sum_{i=0}^{h-2} k^{(1-\theta)i} \quad (50)$$

(ii) For $a \to \infty$, we achieve

$$L_\nu(h,k,n) \approx k^{(h-1)\theta+1} + k^h + \frac{k^h - k^{(h-2)\theta+2}}{k^{1-\theta}-1} \quad (51)$$

Proof: By Taylor's expansion,

$$1-e^{-a} \approx a - \frac{a^2}{2} \quad (52)$$

Substituting the above approximations for $1-e^{-a}$ in Lemma 5 yields the result in (i). The result in (ii) is computed in the limit as $a \to \infty$. Note that $U_\nu^\theta(h,k)$, the average number of links in unicast, is computed by:

$$\begin{aligned} U_\nu^\theta(h,k) &= \frac{1}{M}\sum_{l=1}^{h} k^l \sum_{i=1}^{l} k^{(h-i)\theta} \\ &= k^{h\theta}\left(\frac{1}{k^\theta - 1} - \frac{(k^{(1-\theta)h}-1)(k-1)}{(k^h-1)(k^\theta-1)(k-k^\theta)}\right) \end{aligned} \quad (53)$$

■